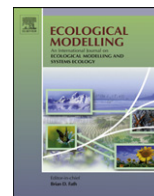




Contents lists available at ScienceDirect

Ecological Modelling

journal homepage: www.elsevier.com/locate/ecolmodel



Estimating California ecosystem carbon change using process model and land cover disturbance data: 1951–2000

Jinxun Liu^{a,*}, James E. Vogelmann^b, Zhiliang Zhu^c, Carl H. Key^d, Benjamin M. Sleeter^e, David T. Price^f, Jing M. Chen^g, Mark A. Cochrane^h, Jeffery C. Eidschink^b, Stephen M. Howard^b, Norman B. Blissⁱ, Hong Jiang^{j,k}

^a Stinger Ghaffarian Technologies (SGT, Inc.)¹, Earth Resources Observation and Science (EROS) Center, 47914 252nd St., Sioux Falls, SD 57198, USA

^b U.S. Geological Survey (USGS) Earth Resources Observation and Science (EROS) Center, 47914 252nd St., Sioux Falls, SD 57198, USA

^c U.S. Geological Survey, 12201 Sunrise Valley Drive, Reston, VA 20192, USA

^d USGS Northern Rocky Mountain Science Center, Glacier Field Station, c/o Glacier National Park, West Glacier, MT 59936-0128, USA

^e U.S. Geological Survey, Western Geographic Science Center, Pacific Geographic Science Team, 345 Middlefield Road MS 531, Menlo Park, CA 94025, USA

^f Natural Resources Canada, Canadian Forest Service (CFS), Northern Forestry Centre, 5320-122 Street, Edmonton, AB, Canada T6H 3S5

^g Department of Geography and Program in Planning, University of Toronto, 100 St. George St., Room 5047, Toronto, Ontario, Canada M5S 3G3

^h Geographic Information Science Center of Excellence (GIScCE), South Dakota State University, 1021 Medary Ave., Wecota Hall, Box 506B, Brookings, SD 57007, USA

ⁱ ASRC Research and Technology Solutions², 47914 252nd Street, Sioux Falls, SD 57198, USA

^j International Center of Spatial Ecology and Ecosystem Ecology, Zhejiang Forestry University, Linan Huanchengbei Road 88, Hangzhou, 311300, China

^k International Institute for Earth System Science, Nanjing University, 22 Hankou Rd., Nanjing 210093, China

ARTICLE INFO

Article history:

Available online xxx

Keywords:

Fire disturbance
Land cover change
CO₂ fertilization
Climate change
IBIS

ABSTRACT

Land use change, natural disturbance, and climate change directly alter ecosystem productivity and carbon stock level. The estimation of ecosystem carbon dynamics depends on the quality of land cover change data and the effectiveness of the ecosystem models that represent the vegetation growth processes and disturbance effects. We used the Integrated Biosphere Simulator (IBIS) and a set of 30- to 60-m resolution fire and land cover change data to examine the carbon changes of California's forests, shrublands, and grasslands. Simulation results indicate that during 1951–2000, the net primary productivity (NPP) increased by 7%, from 72.2 to 77.1 Tg C yr⁻¹ (1 teragram = 10¹² g), mainly due to CO₂ fertilization, since the climate hardly changed during this period. Similarly, heterotrophic respiration increased by 5%, from 69.4 to 73.1 Tg C yr⁻¹, mainly due to increased forest soil carbon and temperature. Net ecosystem production (NEP) was highly variable in the 50-year period but on average equalled 3.0 Tg C yr⁻¹ (total of 149 Tg C). As with NEP, the net biome production (NBP) was also highly variable but averaged -0.55 Tg C yr⁻¹ (total of -27.3 Tg C) because NBP in the 1980s was very low (-5.34 Tg C yr⁻¹). During the study period, a total of 126 Tg carbon were removed by logging and land use change, and 50 Tg carbon were directly removed by wildland fires. For carbon pools, the estimated total living upper canopy (tree) biomass decreased from 928 to 834 Tg C, and the understory (including shrub and grass) biomass increased from 59 to 63 Tg C. Soil carbon and dead biomass carbon increased from 1136 to 1197 Tg C.

Our analyses suggest that both natural and human processes have significant influence on the carbon change in California. During 1951–2000, climate interannual variability was the key driving force for the large interannual changes of ecosystem carbon source and sink at the state level, while logging and fire were the dominant driving forces for carbon balances in several specific ecoregions. From a long-term perspective, CO₂ fertilization plays a key role in maintaining higher NPP. However, our study shows that the increase in C sequestration by CO₂ fertilization is largely offset by logging/land use change and wildland fires.

© 2011 Elsevier B.V. All rights reserved.

* Corresponding author. Tel.: +1 605 594 2806; fax: +1 605 594 6529.

E-mail address: jxliu@usgs.gov (J. Liu).

¹ Contractor to the U.S. Geological Survey, Work performed under USGS contract G10PC00044.

² Contractor to the USGS EROS Center. Work performed under USGS contract G08PC91508.

1. Introduction

Carbon (C) sequestration by ecosystems is an important mechanism to offset the rising atmospheric carbon dioxide (CO₂) concentration resulting from fossil fuel combustion, land use and land cover (LULC) change, and natural ecosystem disturbances. Carbon sequestration by ecosystems tends to increase by CO₂ fertilization and climate change, at least in regions where temperature change increases the growing season length and does not cause additional drought stress (Piao et al., 2006; Girardin et al., 2008; Ju and Chen, 2008). This tendency may be offset by a change in the size, frequency, and intensity of natural disturbances (e.g., wildland fires) and continuing human-induced LULC changes (e.g., logging and deforestation) (Sleeter et al., 2010; Drummond and Loveland, 2010).

Estimating the net C change of ecosystems is affected by the quality of land cover disturbance data and the complexity of the ecosystem models that account for major ecosystem processes (e.g., the growth enhancement effects). In previous years, few regional to global scale modeling studies attempted to address the complicated interactions between climate change, CO₂ fertilization, LULC change, and natural disturbances, mainly due to limited data sources and model capabilities. Now, with new land cover disturbance data products (mostly large datasets from remote sensing) becoming available, there is an increasing need for ecosystem modelers to develop robust ecosystem models and synthesize and incorporate a variety of data into those models. There is also an increasing need for using process-based models instead of empirical models in combination with high-resolution disturbance data to perform long-term large-scale regional C assessment.

California contains parts or all of 12 EPA Level III ecoregions (EPA, 1999). California's diverse geography and relatively high rates of disturbance complicate attempts to track changes in natural C inventories. Previous statewide ecosystem studies, using empirical models or coarse resolution disturbance data, have not provided much detail about the effects of growth enhancement, disturbance, or LULC change (Brown et al., 2004; Mader, 2007; Fried and Zhou, 2008). Process-based modeling studies (Lenihan et al., 2007; Potter, 2010) provided insights on climate change and CO₂ fertilization effect, but they were still limited to coarse resolution and a lack of detailed LULC information.

This study reports on the use of a process-based ecosystem model, the Integrated Biosphere Simulator (IBIS) (Foley et al., 1996), and newly available 30- to 60-m resolution maps of vegetation cover and height (Rollins and Frame, 2006), wildfire severity (Keane et al., 2006; Zhu et al., 2006), and LULC change (Sleeter et al., 2010; Loveland et al., 2002; Stehman et al., 2003) to present a more detailed view of the carbon change of California's natural ecosystems. The purpose of this study is to estimate the effects of CO₂ fertilization and climate change (variability) versus disturbances by wildland fires and LULC changes in terms of net primary production (NPP), net ecosystem production (NEP) derived as NPP – heterotrophic respiration (Rh), and net biome production (NBP) derived as NEP – disturbances (by fires and LULC changes), and to analyze the key drivers of C sequestration in this region. This study focuses on California mainly because the LULC and Monitoring Trends in Burn Severity (MTBS) data products are newly available for this region. Nationwide and global studies will become feasible as new disturbance and LULC data products become available.

2. Materials and methods

IBIS is a process-based biogeochemical model that has been evaluated and applied to many ecosystems (Kucharik et al., 2000;

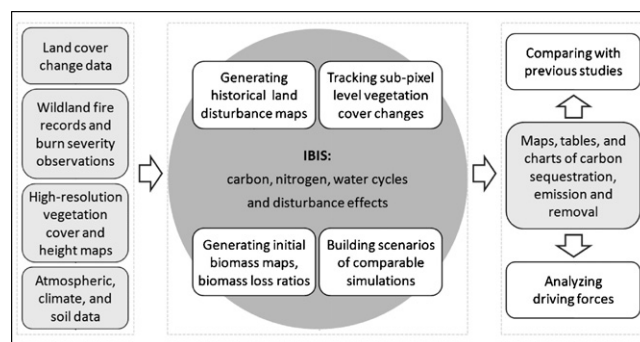


Fig. 1. Conceptual diagram showing the relations among major input data, data processing, model simulation, and post-simulation analyses.

El Mayaar et al., 2001, 2002). We used an extensively modified version with nitrogen controls on soil C decomposition and vegetation growth (Liu et al., 2005), and further incorporated the effects of LULC change and fire disturbances. The overall modeling approach of this study (Fig. 1) includes the following major aspects: (1) initialize vegetation cover and biomass at 1-km resolution using 30-m resolution vegetation data, and track sub-pixel vegetation cover change for each 1-km pixel, (2) intake various land cover change and disturbance information to estimate C removals, including burn severity level processing and related biomass combustion and mortality processing, (3) use process-based algorithms to calculate NPP, NEP, Rh, and NBP, as they are affected by climate and CO₂ fertilizations, and (4) analyze the key drivers of C sequestration using comparable simulations.

2.1. Input data source and data processing

The 30-m resolution vegetation cover and vegetation height data (Fig. S1) were obtained from the LANDFIRE Web site³ and aggregated to 1-km resolution. Each 1-km land pixel had a set of sub-pixel information such as fractional vegetation cover (tree, shrub, grass, non-vegetation, etc.) and empirically calculated initial biomass. The fractional cover of upper canopy (tree) and lower canopy (shrub and grass) constrains upper and lower canopy leaf area index (LAI) of each 1-km land pixel and, therefore, constrains the upper and lower canopy NPP calculation. For example, if environmental conditions (climate and nutrient) allow a maximum tree LAI of 10 on a land pixel but the actual tree fraction is only 0.5, then the actual allowed tree LAI on the pixel will be only about 5. Fractional covers will change depending on land cover disturbances.

Spatially referenced fire records from 1951 to 2000 (Fig. S2) were obtained from the California Department of Forestry and Fire Protection and the USDA Forest Service.⁴ Fire location (perimeter), size, timing, cause, vegetation, etc. were provided in the records. No spatial burn severity information was given. The 30-m resolution LANDSUM (Keane et al., 2006) modeled burn severity maps (Fig. S2) were downloaded from The National Map LANDFIRE viewer – LANDFIRE National Fire Regime.⁵ The three burn severity probability maps were based on potential vegetation type, average climate, topography, and soils. On a 1-km resolution map, area percentages of the three burn severity levels were calculated. When a fire event impacts a land pixel, we assume the vegetation has the same proportional areas of high, medium, and low burn severity as the LANDSUM data.

³ <http://landfire.cr.usgs.gov/viewer/viewer.htm>.

⁴ <http://frap.cdf.ca.gov/data/frapgisdata/select.asp>.

⁵ <http://landfire.cr.usgs.gov/viewer/viewer.htm>.

Data from the MTBS project⁶ were also used. MTBS data for California (1984–2000) include 230 forest fires that were larger than 400 ha. Comparison of the wall-to-wall LANDSUM data and the observed MTBS data showed that the modeled LANDSUM high, medium, and low burn severity classes covered 22%, 23%, and 48% of total reported burned areas, respectively; and the MTBS high, medium, and low burn severity classes were 13%, 21%, and 33% of those forest fires, respectively. The other portions of the fire region were non-burn areas such as barren, road, and water body. A northern California forest fire severity study (Odion et al., 2004) also indicated that the overall fire severity proportions were 12% high, 29% moderate, and 59% low. Therefore, the modeled LANDSUM forest high burn severity percentage was higher than the observed high burn severity in the region. In order to use the wall-to-wall LANDSUM data, we adjusted its forest high burn percentage by reducing it to 70% of its original level (approximately from 22% to 15%).

The 1-km resolution 1992 Global Land Cover Characterization (GLCC) data were obtained from the U.S. Geological Survey (USGS).⁷ The original map has 24 land cover types, which were reclassified into six broad land cover categories: forest, savannah/shrub, grassland, agricultural land, urban, and other nonvegetated land (ice, mining site, barren, etc.). This base map was used to map land cover transitions from 1951 to 2000 (Fig. S3).

The 60-m resolution land cover change data provided by the USGS Land Cover Trends project⁸ (Sleeter et al., 2010) were based on five dates of satellite imagery (1973, 1979, 1986, 1992, and 2000) of 229 sampling blocks (10 × 10 km) (Fig. S3). Land cover transitions between 11 predefined land cover types were regrouped to represent logging, deforestation, devegetation, and other land conversions. These land cover transition rates were applied to the 1992 GLCC reference land cover to create 1973–2000 dynamic 1-km resolution land cover maps. For consistency with fire disturbance simulation, we assume logging and devegetation rates from 1951 to 1972 were the same as those from 1973 to 1979.

The U.S. General Soil Map (STATSGO)⁹ was processed to represent soil profiles containing up to six layers (7, 15, 25, 50, 100, 200 cm depths) with sand, silt, and clay fractions. Total soil organic carbon was also calculated but not allocated to different soil layers (Fig. S4).

The meteorological data from local California weather stations (1951–2000) were interpolated by McKenney et al. (2006) using the ANUSPLIN tool (Hutchinson, 1995) to 30'' (~10-km) resolution (Fig. S5), which accounts for the effects of topography and vegetation type. Monthly climate variables include precipitation, maximum temperature, and minimum temperature. Other climate variables, such as relative humidity and wind speed, are monthly normals for the 1961–1990 period (McKenney et al., 2006). The global atmospheric CO₂ concentration trend was from observed data (Keeling et al., 2001).

Static NH₄ and NO₄ deposition data were downloaded from the National Atmospheric Deposition Program Web site (<http://nadp.sws.uiuc.edu/>) and interpolated to 1-km resolution. The 1-km resolution elevation data were from the global 30-arc-second elevation dataset (GTOPO30).¹⁰

2.2. Productivity calculation methods

The algorithm of leaf photosynthesis in IBIS is a modified Farquhar type model (Farquhar and others, 1980). The gross pho-

tosynthesis rate through light-limited, rubisco-limited, and triose phosphate utilization-limited mechanisms (see Foley et al. (1996), Eqs. (2), (4), and (5)) is partly determined by intercellular CO₂ concentration within the leaf, which is in turn determined by the water conductance and CO₂ concentration at the leaf surface (see Foley et al. (1996), Eqs. (13)–(15)). The gross photosynthesis rate is also modified by leaf nitrogen level, which is determined by soil nitrogen pool (see Liu et al. (2005), Eqs. (1), (8), and (9)). At canopy level, IBIS allows LAI to change dynamically depending on living leaf biomass. The biomass mortality rate is simplified by using constant turnover ratios for each vegetation type and each biomass component (leaf, roots, stems, etc.). However, when disturbances are considered, additional mortality or biomass loss is calculated. For example, when fire happens, live forest biomass is allocated to direct combustion, additional mortality (dead tree wood by fire), and remaining live biomass, depending on burn severity.

In this study, a majority of the 1-km land pixels was a mixture of forest, shrub, grass, and non-vegetation land covers based on the 30-m land cover maps. We assume their area proportions in the 1-km pixel would not change much unless disturbance happens. Therefore, we have introduced physical limits of vegetation fractional cover so that effective forest, shrub, and grass covers (area percentage) help provide more realistic photosynthesis rates. Disturbance events can affect one or more of the land covers. Sub-pixel vegetation fractions were adjusted following various disturbance events, like deforestation, reforestation, and urbanization. For example, deforestation activity is assumed to remove trees permanently and will reduce forest cover to 5% with the land cover type no longer being a forest; reforestation will restore tree cover up to 80% on non-forest vegetated land within a 1-km pixel and reduce shrub and grass cover accordingly.

2.3. Soil organic carbon (SOC) initialization

Soil C pool initialization in IBIS is based on a spin-up process and soil survey data. The usual spin-up performs additional soil cycles (in IBIS, up to 40 times) for each ordinary soil cycling step so that all soil pools can reach a quasi-equilibrium. Although the SOC pools can be balanced, this process usually brings an unrealistic total SOC pool size compared to field data. By analyzing and testing the IBIS soil C module, we found that the slow SOC pool is almost linearly proportional to the NPP level whereas the passive SOC is not. Through testing, we also found that a 5 kg C m⁻² slow SOC pool size is usually enough to support a locally high level NPP output. Considering that some locations have higher total soil C stock (>10 kg C m⁻²), we first set up an initial slow SOC pool (50% of total surveyed SOC value but no larger than 5 kg C m⁻²) and then deducted the slow SOC from the total SOC to initialize the passive SOC pool. However, a maximum amount of the passive SOC (10 kg C m⁻²) was allowed to participate in the soil decomposition process to help avoid excessive decomposition of passive SOC. This is especially useful for maintaining a total SOC level when the input total soil C pool is big (e.g., 30 kg C m⁻² or more). The extra passive SOC was assumed inactive within a year, but can be modified between years. If reactive passive SOC decreased, we allow the inactive passive SOC to compensate for the loss; if reactive passive SOC increased (i.e., more than 10 kg C m⁻²), we will move the newly gained C to the inactive passive SOC pool. We also introduced soil priming effect, which helped to stabilize the soil pools (Liu et al., 2005). The active SOC pool was set at 2% of total SOC, or 0.5 kg C m⁻² at the maximum. Because of the fast turnover rate, the active SOC pool will quickly find its balance level after several years of simulation.

⁶ <http://svinetfc4.fs.fed.us/mtbs/index.html>.

⁷ <http://edcsns17.cr.usgs.gov/glcc/na.int.html>.

⁸ <http://edc2.usgs.gov/LT/>.

⁹ <http://www.ncgc.nrcs.usda.gov/products/datasets/statsgo/>.

¹⁰ <http://eros.usgs.gov/products/elevation/gtopo30/gtopo30.html>.

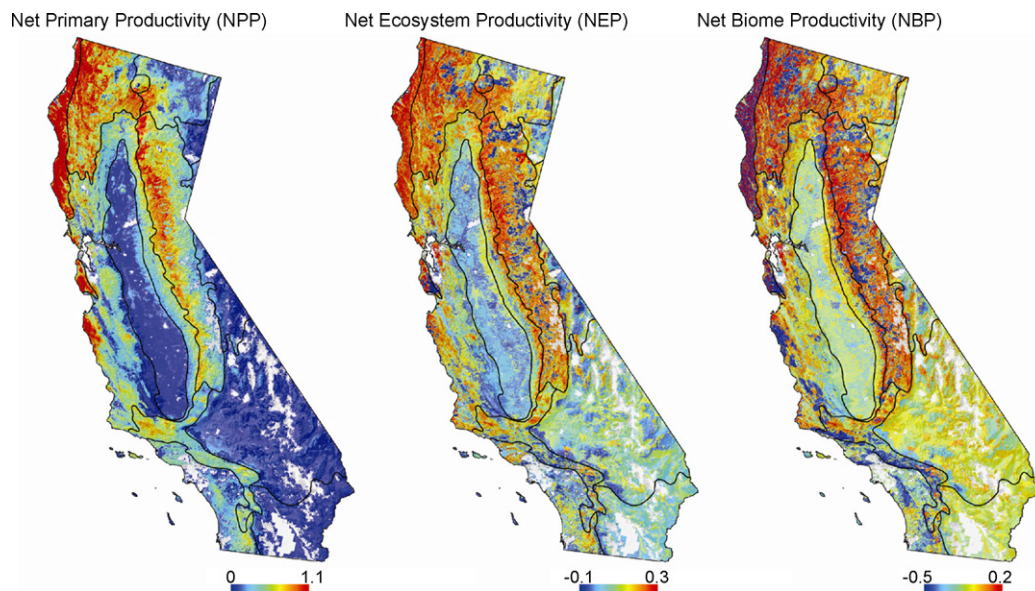


Fig. 2. Spatial distributions of the net primary productivity (NPP), net ecosystem productivity (NEP) and net biome productivity (NBP) of natural ecosystems of California as affected by fire, land cover change, and growth enhancement. Values are averages of 50 years (1951–2000). Unit is $\text{kg C m}^{-2} \text{ yr}^{-1}$.

2.4. Initial biomass carbon at 1-km resolution

We used the 30-m resolution canopy cover and tree height to initialize biomass at 1-km resolution:

$$B = \frac{\sum_{i=1}^{N_f} (C_i * B_h / A)}{N_0} \quad (1)$$

where B is the averaged biomass density in a 1-km pixel; C_i is the 30-m tree canopy cover that varies from 10% to 100% (nine levels); A is the reference canopy cover (70%); B_h is the reference biomass C at five tree height levels, which is shown in Table 1; N_f is the total 30-m forested pixels ($C_i > 10\%$), and N_0 is the total 30-m pixels in a 1-km cell.

On the other hand, we used 30-m land cover information to estimate the effective fractional vegetation cover within each 1-km land pixel. The fractional cover of forest at 1-km resolution is

Table 1
 Arbitrary aboveground tree/shrub biomass setup with 70% canopy cover. Numbers in brackets indicate the height range.

Tree height (m)	0–5	5–10	10–25	25–50	>50
Tree biomass (kg C/m^2)	2	4	8	16	30
Shrub height (m)	0–0.5	0.5–1.0	1–2	2–4	
Shrub biomass (kg C/m^2)	0.5	1	1.5	3	

calculated as:

$$P_f = \frac{N_f}{N_0} \quad (2)$$

$P_f = 0.6$ means that a 1-km land pixel has 60% area being classified as forest. The rest could be road, water body, barren, farmland, developed land, etc. The actual canopy cover (or canopy closure) of those forests theoretically can vary from 10 to 100%. When disturbances are considered, fractional cover of forest will be changed

Table 2
 Combustion and/or mortality ratios of biomass and soil organic matter at different burn severity levels. Litter/fine fuel combustion ratios apply to dead leaf and dead root pool; medium fuel combustion ratios apply to woody litter pool. The values for soil combustion represent the area percentage of bare soil exposed after fire.

Components	Combustion (%)			Mortality (%)		
	Low	Moderate	High	Low	Moderate	High
Forest floor and soil						
Litter/fine fuel	15–60	61–90	91–100			
Duff	5–30	31–70	71–100			
Medium fuel	10–30	31–50	51–100			
Heavy	5–15	16–40	41–100			
Soil	5–20	21–50	51–100			
Understory layer						
Herb	15–60	61–65	86–100			
Shrub-leaf-wood	10–40	41–60	61–100			
Shrub-leaf-wood				1–20	21–70	71–100
Pie_mature trees						
Leaf	1–20	21–70	71–100			
Fine branch	1–20	21–70	71–100			
Wood				1–20	21–75	76–100
Mature trees						
Leaf	1–20	21–70	71–100			
Branch	1–20	21–70	71–100			
Wood				1–20	21–70	71–100

accordingly. For deforestation and desegregation, P_f will be set to zero.

Similar calculations of shrub biomass and grass biomass are also included in the model based on height and reference biomass (Table 1) and fractional cover.

2.5. Quantification of CO₂ fertilization and climate change effects

Analyses of CO₂ fertilization and climate change effects were based on comparative simulation experiments: (1) Climate_Only, using 1951–2000 historical monthly climate data with CO₂ concentration held constant at the 1950 level (308 ppm); (2) CO₂_Only, using 1961–1990 average climate and observed CO₂ concentration data; (3) Climate+CO₂, using historical climate and observed CO₂ concentration data; and (4) CO₂_Conservative, an adjusted calculation that gave lower CO₂ fertilization effect. We used the Climate+CO₂ simulation minus the Climate_Only simulation and the CO₂_Conservative simulation minus the Climate_Only simulation to quantify the CO₂ effects; we also used the Climate+CO₂ simulation minus the CO₂_Only simulation to analyze the climate change effects.

The CO₂_Conservative simulation was implemented because considerable variability of the CO₂ fertilization effect (0–60%) under the doubled CO₂ concentration scenario has been noted (Running, 2008) and the “progressive nutrient limitation” may also be incurred as CO₂ concentration increases (Luo et al., 2004). The CO₂ increase during 1951–2000 was about 20%, so we targeted our conservative CO₂ effect to be around 6–7% of NPP increase. The CO₂_Conservative model experiment used an exponential decay function to reduce the CO₂ effect:

$$C_{sa}(t) = C_{sa}(t-1) + (C_s(t) - C_s(t-1)) * e^{-0.03(t-1950)} \quad (3)$$

where C_{sa} is the adjusted CO₂ concentration that replaces C_s (actual CO₂ concentration at the leaf surface) to calculate the photosynthesis rate; and t is the calendar year (>1950). Coefficient -0.03 is arbitrary, which gives about half of the CO₂ fertilization effect calculated by the non-conservative model experiment for 1951–2000.

2.6. Quantification of land cover change effects

For the stand-replacing logging events, 70% of aboveground woody biomass C was assumed to be removed from the ecosystem (Brown et al., 2004; Arora and Boer, 2005). The remaining 30% of aboveground woody biomass C could be allocated to dead biomass (i.e., logging-induced mortality). But we also added this portion to C removal assuming it will be burned after harvesting. Forest was assumed to regenerate the next year. For the devegetation event (e.g., urbanization), we assumed that all living biomass was removed from the system with no vegetation regrowth. The LULC transition rates were derived from the Land Cover Trends data (Table S1) (Sleeter et al., 2010). Location of forest logging within each ecoregion was set randomly based on the annual logging rates and only on forested land pixels; deforestation and devegetation were set semi-randomly using the 1992 1-km resolution land cover grids where the rate of change was applied to pixels at land cover type boundary lines. Fractional vegetation cover (trees, shrubs, and grasses) on each 1-km pixel was adjusted following deforestation and devegetation events.

2.7. Quantification of fire disturbance effects

Effects of fire disturbance on C loss were calculated using fire area, burn severity, and biomass loss ratios. For fire area, we chose wildland fires larger than 0.8 km² (200 acres) in the fire database.

For burn severity levels, on each 1-km resolution land pixel, the area percentages of the high, medium, and low burn levels were calculated from the LANDSUM 30-m resolution burn severity probability data and used as weights in the carbon loss calculation. The high burn weight from LANDSUM was adjusted using MTBS data and field observation data.

The ratio of biomass and soil combustion and the ratio of fire-induced vegetation mortality were generated from the correlations between the satellite-based Differenced Normalized Burn Ratio (DNBR) product of the MTBS project and the Composite Burn Index (CBI), which is a commonly collected ground-based variable to estimate postfire effects. These specific combustion and/or mortality ratios for tree, shrub, grass, surface fine litter, and soil organic matter are listed in Table 2, which was based on field data from over 80 burns (collected by C. Key et al., USGS).

2.8. Simulation setup

Model simulations were from 1901 to 2000 at 1-km spatial resolution. 1901–1950 was the soil spin-up period by which we let the model establish relatively balanced soil carbon pools. Soil textures and soil profile properties were assumed not to change. We only report the simulation results from 1951 to 2000.

A Beowulf cluster computer was used to run the model. California was divided into 930 subregions (i.e., 930 lines from north to south at approximately 1-km resolution). Each subregion was independently simulated at 1-km spatial resolution with 30–60-m resolution subpixel information, and then aggregated into the whole region.

3. Results

3.1. Disturbance induced carbon loss and ecosystem productivity

State level disturbance areas and related C changes are shown in Table 3. Logging activities peaked in the 1980s, and natural wildland fires were highest in the 1990s. Total combustion (of biomass, litter, and soil organic matter) increased from the 1950s to the 1990s, averaging 1.01 Tg C yr⁻¹ (1 teragram = 10¹² g). However, fire-induced carbon loss did not strictly scale with the total area burned. For example, carbon emissions per unit fire area for the 1980s were 18% higher than those for the 1990s because combustion releases are a function of carbon stock (fuel level) and burn severity. Our spatially explicit biomass and burn severity data helped to quantify this variability. Estimated C losses due to LULC change (removal plus deforestation and devegetation) also increased between 1951 and 2000, averaging 2.51 Tg C yr⁻¹. The average loss per unit area was 101.5 Mg C ha⁻¹, approximately 10 times the amount directly lost from fires (9.4 Mg C ha⁻¹). This difference occurred because most fires were not stand-replacing, and many were in regions carrying low biomass densities, notably shrublands. Simulated NPP and Rh increased during the 1950s–1990s, averaging 74.2 and 71.3 Tg C yr⁻¹, respectively. Total increase in NPP was about 7% within 50 years. The NEP and NBP, which averaged 3.0 and -0.55 Tg C yr⁻¹, respectively, and did not show a consistent increase. NEP and NBP became very low during the 1980s (0.4 and -5.34 Tg C yr⁻¹, respectively) because of increased disturbances and drier climate conditions. The 1-km resolution maps of 50-year average of NPP, NEP and NBP are shown in Fig. 2. Ecoregion level C balances are summarized in Fig. 3. Most of the larger C fluxes appeared on forested ecoregions.

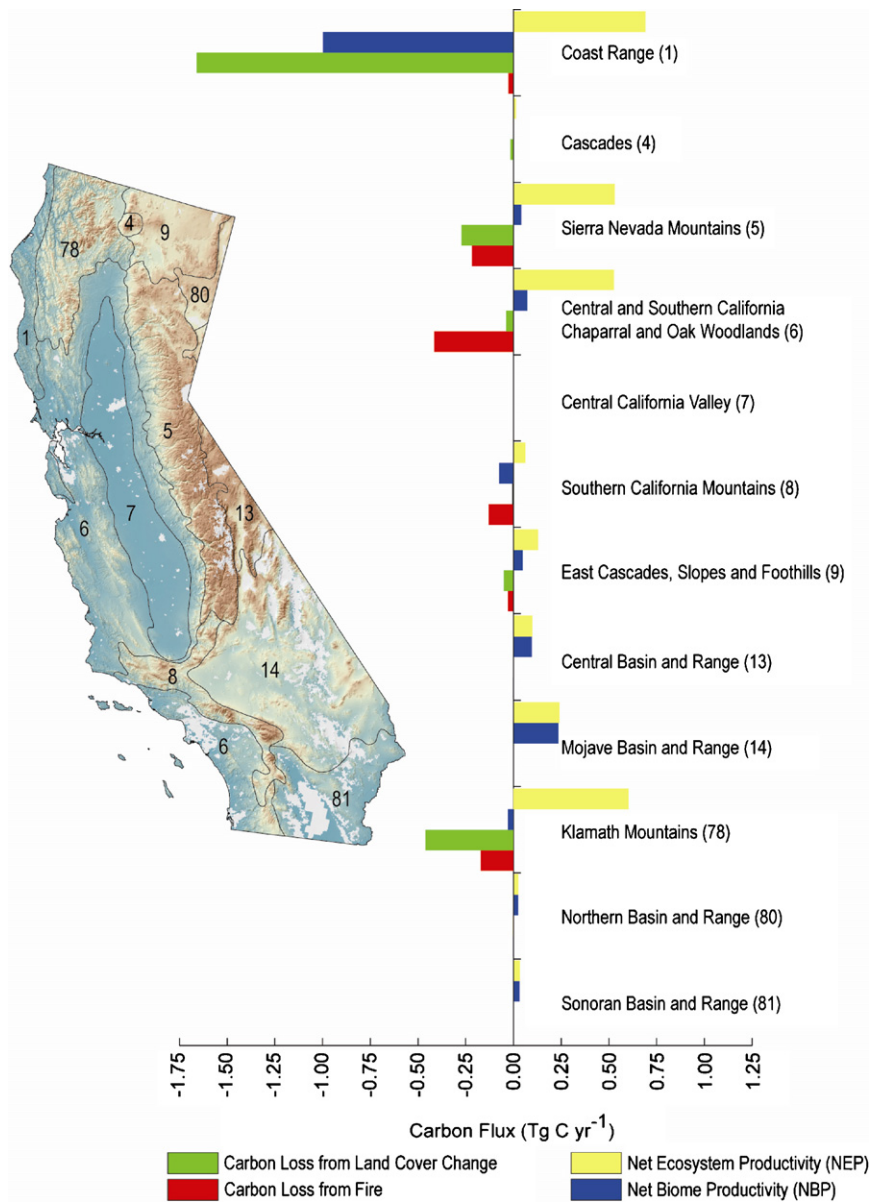


Fig. 3. Estimated annual carbon loss from ecosystem disturbances (wildfires, forest harvesting, deforestation, devegetation) and ecosystem productivity of Californian ecoregions. NBP equals NEP minus carbon removal from fire and LULC change. Agricultural lands were not simulated in the study.

3.2. Growth enhancement effects

Observed atmospheric CO₂ concentration increased by 20% during 1951–2000. NPP increase with non-conservative CO₂ fertilization (Climate + CO₂ simulation minus the Climate.Only simulation) was about 9 TgC, or 11% of the 1950s level. This CO₂ fertilization effect is comparable to that reported for Free Air CO₂ Enrichment (FACE) experiments in North America and Europe (NPP increase: 23–25% and CO₂ increase: 46%) (Norby et al., 2005; Hickler et al., 2008) and to the results of a tree ring study in California (relative tree radial growth increase: 15–25%, before 1950s vs. after 1950s) (Soulé and Knapp, 2006). However, the CO₂.Conservative simulation indicated that with reduced CO₂ forcing, NPP would only increase by 4.9 TgC, or 7% relative to the 1950s level. This magnitude is higher than a modeling study by Lenihan et al. (2007), where the CO₂ fertilization effect on NPP is about a 6% increase under a 33% CO₂ concentration increase. Model simulation indicated that even though growth enhancement raises NPP, it may not necessarily raise or maintain NEP (Fig. 4a). Simulated NPP also

showed a slight increasing trend in response to climate change during 1951–2000. Yet NEP did not show an obvious increase (Fig. 4b).

Despite growth enhancement, average NPP in the 1990s was lower than that of 1980s because of land disturbances and unfavorable climate. The mean and variation of the simulated NPP (CO₂.Conservative scenario) in different ecoregions are shown in Fig. S6. Comparisons of simulated NPP with other studies are listed in Table S2. In general, our simulated NPP fell within the range of available field observations and regional studies.

3.3. Carbon stock change and dominant driver of carbon balance

During 1951–1983, simulated total living biomass C slightly decreased from 993 Tg to 963 Tg (1 Tg C yr⁻¹) while total soil and dead biomass C increased from 1123 Tg to 1203 Tg (2.5 Tg C yr⁻¹). Total ecosystem carbon was increasing. From 1984 to 1991, due to disturbance, LULC change, and unfavorable climate, living biomass C decreased from 963 to 896 Tg (approximately 10 Tg C yr⁻¹) and soil C remained unchanged. Total ecosystem C decreased signif-

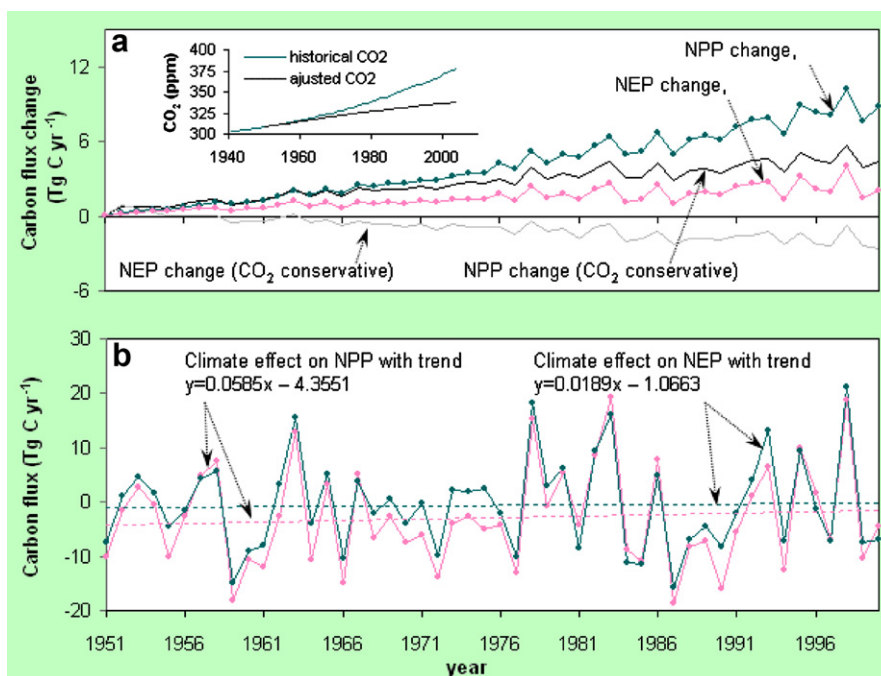


Fig. 4. Growth enhancement effects on net primary productivity (NPP) and net ecosystem productivity (NEP). Carbon flux change is quantified by comparative simulations. (a) CO₂ fertilization effect: the CO₂-Conservative scenario used an adjusted CO₂ input by which actual CO₂ fertilization was assumed to become progressively limited since 1951. Although the conservative scenario promoted an increase in NPP, it did not promote an increase in NEP. (b) Climate change effect: Although NPP showed a slight increasing trend, NEP did not show an obvious increase.

icantly. After 1991, living biomass basically remained stable and soil C began to accumulate (Fig. 5).

Annual direct C losses due to disturbances varied between -1.6 and $-11.6 \text{ Tg C yr}^{-1}$ (mean = $-3.5 \pm 2.0 \text{ Tg C yr}^{-1}$). A minus sign indicates C removal from the ecosystem. The error term is the interannual variability. However, NBP varied from -14.7 to $+15.0 \text{ Tg C yr}^{-1}$ (mean = $-0.55 \pm 7.1 \text{ Tg C yr}^{-1}$). This indicates that climate variability contributed more than disturbances to inter-annual fluctuations in the statewide C balance (Fig. 5). Further statistical analysis (Table S3) shows that annual precipitation is strongly and positively correlated with NEP and NBP, while temperature is correlated positively with soil Rh and negatively with NPP,

NEP, and NBP. LULC change and fire have relatively small impacts on NBP fluctuation at the state level but can be dominant at the ecoregion level (e.g., Coast Range and Sierra Nevada).

The grassland/shrub-dominated Chaparral and Oak Woodlands ecoregion (ecoreg #1) is the most populated ecoregion in California, yet increasing urbanization is not a major driving factor of ecosystem carbon loss. Instead, wildfire is the key driver. This ecoregion had the largest fraction of fire-induced carbon loss while the remainder came largely from ecoregions dominated by forest cover (i.e., Sierra Nevada (ecoreg #5), Klamath Mountains (ecoreg #78), and Southern California Mountains (ecoreg #8)). The forest-dominated ecoregions lost a large amount of carbon due to LULC

Table 3

Decadal averages of annual disturbance areas, disturbance carbon loss, ecosystem heterotrophic respiration, and ecosystem productivity of California ecosystems from the all-included simulation. (NPP – net primary productivity; NEP – net ecosystem productivity; NBP – net biome productivity).

	1950s	1950s	1970s	1980s	1990s	Average	Total (50 yr)
Disturbance area (km ² yr ⁻¹)							
Total fire area	1021	959	910	1200	1274	1073	53,648
Average fire size	0.9	1.2	1.0	1.2	1.4	1.1	
Logging			87	235	161	161	8042
Deforestation			5	3	6	7	342
Devegetation			57	123	57	73	3957
Carbon loss (Tg C yr ⁻¹)							
Combustion	1.17	0.81	0.85	1.17	1.06	1.01	50
Veg. mortality (by fire)	1.00	0.69	0.71	0.98	0.86	0.85	42
Logging	1.43	1.47	1.6E	4.49	3.15	2.44	122
Deforestation			0.01	0.02		0.01	0.6
Devegetation	0.01	0.01	0.06	0.12	0.12	0.07	3.3
Heterotrophic respiration (Rh)	69.4	70.0	70.2	73.7	73.1	71.3	3564
Productivity (Tg C yr ⁻¹)							
Net primary productivity (NPP)	72.2	73.2	74.7	74.2	77.1	74.2	3712
Net ecosystem productivity (NEP)	2.8	3.2	4.5	0.4	4.0	3.0	149
Net biome productivity (NBP)	0.14	0.90	1.88	-5.34	-0.31	-0.55	-27.3
Carbon pools (Tg C)							
Tree biomass C	928	909	897	874	834	888	
Shrub and grass biomass C	59	59	60	61	63	60	
Soil and dead biomass C	1136	1156	1172	1191	1197	1171	
Total ecosystem C	2123	2126	2129	2127	2093	2119	

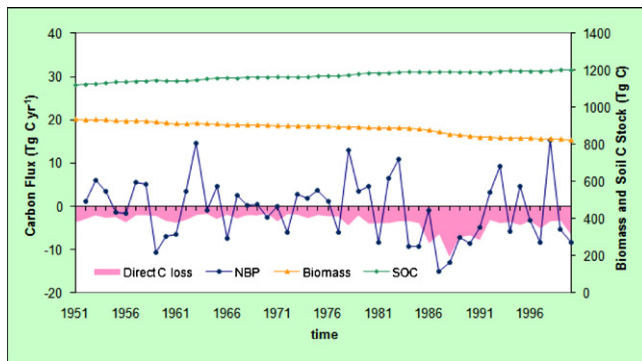


Fig. 5. Estimated carbon stock in soil and forest biomass, carbon loss due to disturbances, and net biome productivity (NBP) in California.

changes (primarily logging). The Coast Range ecoregion (ecoreg #1) was a carbon source because of high carbon removals due to relatively high rates of logging. Although grassland/shrub-dominated ecoregions account for nearly 25% of the area affected by LULC change, they did not contribute much to carbon loss because they are characterized by low biomass densities.

4. Discussion

It is difficult to compare our studies with other research in other regions because detailed, regional, high-resolution LULC information is not readily available for C modeling at present. Therefore, we focus on comparing some previous California statewide C research and assessments such as forest inventory-based studies (Birdsey and Lewis, 2003; Brown et al., 2004; Christensen et al., 2008; Mader, 2007; Fried and Zhou, 2008) and process-based modeling studies combined with remote sensing and/or forest inventory (Lenihan et al., 2007; Potter, 2010). The inventory-based studies focused on a short time period, mostly from the 1980s to 1990s or the early 2000s. Our estimate of average NBP for California in the 1990s was $-0.31 \text{ Tg C yr}^{-1}$, which is lower than a California baseline forest and rangeland NBP estimate of $2.52 \text{ Tg C yr}^{-1}$ (Brown et al., 2004) and another forest inventory-based estimate of $2.68 \text{ Tg C yr}^{-1}$ (forest land only) (Birdsey and Lewis, 2003). Many factors could have caused this difference. First, our assumptions on stand-replacing disturbances (e.g., logging and deforestation) may have caused higher C removal. A portion of the remaining live biomass should be considered in the model, and slashes that were assumed to be removed or burned after cutting should also keep a proportion in the ecosystem too. Second, the logging locations across the landscape were randomly allocated in forested areas in this study. Obviously some old-growth and protected forest areas were affected by this simplification. Those areas usually have a high level of C stock, hence they had a high C removal if logging occurred. Third, our NPP calculations used a conservative formulation of CO_2 fertilization. Setting a higher CO_2 fertilization effect will narrow the difference. However, our NPP magnitude is comparable to some field and modeling studies (e.g., Huduburg et al., 2009) (Table S2). In addition, differences in fractional vegetation cover calculation and baseline biomass stock levels would also contribute to the differing results. In Table 1 we listed our initial biomass calculation assuming a reference forest cover average at 70%. If we lower the value to 60%, based on biomass calculation (Eq. (1)), total initial biomass will be increased and total C removal and mortality will also be increased. Certainly, this reference forest cover is an uncertainty area that should be resolved. We also identified other modeling aspects that need improvements, such as the mortality rate of old growth forest and dead biomass initialization. Further comparisons

with forest inventory-based results at various spatial scales will be helpful to reduce model uncertainty.

On the process modeling aspects, our estimated NBP range as affected by climate variability, CO_2 fertilization, and disturbance (-14.7 to $+15.0 \text{ Tg C yr}^{-1}$) is close to the results of Potter (2010) that net ecosystem C flux fell in the range of -15 to $+24 \text{ Tg C yr}^{-1}$. Our estimated NPP ranges are also comparable to some local studies (Table S2). The estimated 7% NPP increase due to CO_2 fertilization during 1951–2000 is relatively comparable to the study of Lenihan et al. (2007) and some other studies as discussed in Section 3.2, although this is still a highly uncertain area. Growth enhancements due to CO_2 fertilization and recent climate warming help to offset C emissions associated with increased disturbance from wildfire and LULC change and have therefore maintained a positive average NEP and basically a neutral average NBP for California's natural ecosystems. Regardless, based on CO_2 fertilization analysis, even though CO_2 fertilization and climate change may allow NPP to increase in future years, ecosystem NEP may eventually decline because the increases in ecosystem respiration could exceed the increases in NPP. It is also noticeable that natural disturbance (fire) has also increased in size and intensity in recent years, which adds another acceleration factor in C release from ecosystems. This means that extra C gains from growth enhancement could be wasted through enhanced ecosystem respiration and natural disturbances. This will provide implications to land managers in understanding the ecosystem response to climate change and land use activities.

Acknowledgments

This study was supported by the USGS LANDFIRE project at USGS EROS. We thank the researchers from the Land Cover Trends project and the Monitoring Trends in Burn Severity project for data and technical assistance. Carol Deering assisted in reference search and citation. Thomas Adamson conducted a technical edit.

Appendix A. Supplementary data

Supplementary data associated with this article can be found, in the online version, at doi:10.1016/j.ecolmodel.2011.03.042.

References

- Arora, V.K., Boer, G.J., 2005. Fire as an interactive component of dynamic vegetation models. *J. Geophys. Res.* 110, G02008, doi:10.1029/2005JG000042.
- Birdsey, R.A., Lewis, G.M., 2003. Carbon in U.S. forests and wood products, 1987–1997 State-by-state estimates. General technical report NE, 310. USDA Forest Service, Northeastern Research Station, Newtown Square, PA.
- Brown, S., Pearson, T., Dushku, A., Kadyzewski, J., Qi, Y., 2004. Baseline Greenhouse Gas Emissions and Removals for Forest, Range, and Agricultural Lands in California. Winrock International, for the California Energy Commission, PIER Energy-Related Environmental Research. 500-04-069F.
- Christensen, G.A., Campbell, S.J., Fried, J.S., 2008. California's forest resources, 2001–2005: five-year Forest Inventory and Analysis report. Gen. Tech. Rep. PNW-GTR-763. 183 p.
- Drummond, M.A., Loveland, T.R., 2010. Land-use pressure and a transition to forest-cover loss in the eastern United States. *Bioscience* 60 (4), 286–298.
- El Mayaar, M., Price, D.T., Delire, C., Foley, J.A., Black, T.A., Bessemoulin, P., 2001. Validation of the integrated biosphere simulator over Canadian deciduous and coniferous boreal forest stands. *J. Geophys. Res.* 106, 14,339–14,355.
- El Mayaar, M., Price, D.T., Black, T.A., Humphreys, E.R., Jork, E.-M., 2002. Sensitivity tests of the integrated biosphere simulator to soil and vegetation characteristics in a Pacific coastal coniferous forest. *Atmos. Ocean* 40, 313–332.
- EPA, 1999. Level III Ecoregions of the Continental United States. (1:7,500,000-scale map). Corvallis, Oregon: U.S. Environmental Protection Agency, National Health and Environmental Effects Research Laboratory.
- Farquhar, G.D., von Caemmerer, S., Berry, J.A., 1980. A biochemical model of photosynthetic CO_2 assimilation in leaves of C3 species. *Planta* 149, 78–90, doi:10.1007/BF00386231.
- Foley, J.A., Prentice, I.C., Ramankutty, N., Levis, S., Pollard, D., Sitch, S., Haxeltine, A., 1996. An integrated biosphere model of land surface process, terrestrial carbon balance and vegetation dynamics. *Global Biogeochem. Cycles* 10, 603–628.

- Fried, J.S., Zhou, X., 2008. Forest inventory-based estimation of carbon stocks and flux in California forests in 1990. USDA Forest Service – General Technical Report PNW-GTR(750), pp. 1–27.
- Girardin, M.P., Raulier, F., et al., 2008. Response of tree growth to a changing climate in boreal central Canada: a comparison of empirical, process-based, and hybrid modelling approaches. *Ecol. Model.* 213 (2), 209–228.
- Hickler, T., et al., 2008. CO₂ fertilisation in temperate forest FACE results not representative for global forests. *Global Change Biol.* 14, 1531–1542.
- Huduburg, T., et al., 2009. Carbon dynamics of Oregon and Northern California forests and potential land-based carbon storage. *Ecol. Appl.* 19, 163–180.
- Hutchinson, M.F., 1995. Interpolating mean rainfall using thin plate smoothing splines. *Int. J. GIS* 9 (4), 385–403.
- Ju, W., Chen, J.M., 2008. Simulating the effects of past changes in climate, atmospheric composition, and fire disturbance on soil carbon in Canada's forests and wetlands. *Global Biogeochem. Cycles* 22 (GB3010).
- Keane, R.E., Holsinger, L.M., Pratt, S.D., 2006. Simulating historical landscape dynamics using the landscape fire succession model LANDSUM version 4.0. Gen. Tech. Rep. RMRS-GTR-171CD, 73 pp., U.S. Department of Agriculture, Forest Service, Rocky Mountain Research Station, Fort Collins, CO.
- Keeling, C.D., et al., 2001. Exchanges of atmospheric CO₂ and ¹³CO₂ with the terrestrial biosphere and oceans from 1978 to 2000. I. Global aspects, SIO Reference Series, No. 01-06, Scripps Institution of Oceanography, San Diego, 88 p.
- Kucharik, C.J., et al., 2000. Testing the performance of a dynamic global ecosystem model: water balance, carbon balance, and vegetation structure. *Global Biogeochem. Cycles* 14, 795–825.
- Lenihan, J.M., Bachelet, D., et al., 2007. Response of vegetation distribution, ecosystem productivity, and fire to climate change scenarios for California. *Climatic Change*, 1–16.
- Liu, J., Price, D.T., Chen, J., 2005. Nitrogen controls on ecosystem carbon sequestration: a model implementation and application to Saskatchewan, Canada. *Ecol. Model.* 186, 178–195.
- Loveland, T.R., Sohl, T.L., Stehman, S.V., Gallant, A.L., Saylor, K.L., Napton, D.E., 2002. A strategy for estimating the rates of recent United States land-cover changes. *Photogramm. Eng. Rem. S.* 68 (10), 1091–1099.
- Luo, Y.Q., et al., 2004. Progressive nitrogen limitation of ecosystem responses to rising atmospheric carbon dioxide. *Bioscience* 54, 731–739.
- Mader, S., 2007. Climate project: carbon sequestration and storage by California forests and forest products. Tech. Memorandum. Forests for the next century, 34 pp. (online) <http://www.foresthealth.org/pdf/CH2M%20Hill%20Forest%20Carbon%20Study.pdf>.
- McKenney, D., Price, D., Papadopol, P., Siltanen, M., Lawrence, K., 2006. High-resolution climate change scenarios for North America. Frontline Technical Note No. 107, 6 pp., Can. For. Serv. Great Lakes Forestry Centre, Sault Ste. Marie.
- Norby, R.J., et al., 2005. Forest response to elevated CO₂ is conserved across a broad range of productivity. *Proc. Natl. Acad. Sci. U.S.A.* 102, 18052–18056.
- Odion, D.C., Frost, E.J., Strittholt, J.R., Jiang, H., Dellasala, D.A., Morize, M.A., 2004. Patterns of fire severity and forest conditions in the Western Klamath mountains, California. *Conserv. Biol.* 18, 927–936.
- Piao, S.L., Friedlingstein, P., 2006. Effect of climate and CO₂ changes on the greening of the northern hemisphere over the past two decades. *Geophys. Res. Lett.* 33 (23), 23402, Art. No. L23402.
- Potter, C., 2010. The carbon budget of California. *Environ. Sci. Policy* 1, 36–54.
- Rollins, M.G., Frame, C.K., 2006. The LANDFIRE Prototype Project: Nationally consistent and locally relevant geospatial data for wildland fire management. Tech. Rep. RMRS-GTR-175, 416 pp., USDA Forest Service, Rocky Mountain Research Station, Fort Collins, CO.
- Running, S.W., 2008. Ecosystem disturbance, carbon, and climate. *Science* 321, 652.
- Sleeter, B.M., Wilson, T.S., Souldard, C.E., Liu, J., 2010. Estimation of late twentieth century land-cover change in California. *Environ. Monit. Assess.*, doi:10.1007/s10661-010-1385-8.
- Soulé, P.T., Knapp, P.A., 2006. Radial growth rate increases in naturally occurring ponderosa pine trees: a late-20th century CO₂ fertilization effect? *New Phytol.* 171, 379–390.
- Stehman, S.V., Sohl, T.L., Loveland, T.R., 2003. Statistical sampling to characterize recent United States land-cover change. *Remote Sens. Environ.* 86, 517–529.
- Zhu, Z., Key, C.H., Ohlen, D., Benson, N., 2006. Evaluate Sensitivities of Burn-Severity Mapping Algorithms for Different Ecosystems and Fire Histories in the United States. Final Report to the Joint Fire Science Program, Project JFSP 01-1-4-12, 35 pp.